ELSEVIER

Contents lists available at ScienceDirect

Electrochimica Acta

journal homepage: www.elsevier.com/locate/electacta



In-situ electrochemical formation of nickel oxyhydroxide (NiOOH) on metallic nickel foam electrode for the direct oxidation of ammonia in aqueous solution



Yu-Jen Shih a, **, Yao-Hui Huang b, C.P. Huang c, *

- ^a Institute of Environmental Engineering, National Sun Yat-sen University, Kaohsiung, 804, Taiwan
- ^b Department of Chemical Engineering, National Cheng-Kung University, Tainan, 701, Taiwan
- ^c Department of Civil and Environmental Engineering, University of Delaware, Newark, DE, 19716, USA

ARTICLE INFO

Article history: Received 1 March 2018 Received in revised form 27 May 2018 Accepted 27 May 2018 Available online 28 May 2018

Keywords: NiOOH Ammonia oxidation Voltammetry Constant current Nitrogen selectivity

ABSTRACT

A nickel foam-supported Ni(OH)₂/NiOOH electrode, synthesized *in-situ* at a specific electrode overpotential, was used to study the oxidation of ammonia in aqueous solution. Results of voltammetric analysis showed the formal potential of Ni(OH)₂/NiOOH transition at +0.6 V (vs. Hg/HgO, pH 11) at which the current profile was improved by electron transfers of NH₃ in the electrolyte. Selectivity of NH₃ conversion to NO $_{3}^{-}$ and N₂ was evaluated by batch constant current experiments. Electrochemical parameters, including solution pH (6–12), temperature (20–40 °C), current density (0.2–3 mA cm $^{-2}$), and initial NH₃-N concentration (20–450 mg-L $^{-1}$), that may affect ammonia oxidation toward nitrogen selectivity were studied. At constant current density of 1.5 mA cm $^{-2}$ A, ammonia removal reached 98.5% and NO $_{3}^{-}$ was the major product at initial NH₃-N concentration of 50 mg-L $^{-1}$ in 7 h. By contrast, N₂ evolution dominated at low current density (<1 mA cm $^{-2}$) and high initial NH₃-N concentration (i.e., >100 mg-L $^{-1}$). A surface steady-state approach, with NH₃ deprotonation as the rate-limiting step, provided the reaction pathways of NH₃ conversion to molecular nitrogen byproduct.

 $\ensuremath{\text{@}}$ 2018 Elsevier Ltd. All rights reserved.

1. Introduction

Inorganic nitrogen species (e.g., nitrate, nitrite, and ammonia) are major micro-nutrients that contribute to water eutrophication [1]. Ammonium/ammonia is the main byproduct when numerous nitrogenous organic compounds, such as azo dyes, organic solvents, and pharmaceutical products, are degraded at wastewater treatment plants (WWTP), especially those receive waste discharges from the high-tech industries [2]. The Urban Waste Water Directive (92/271/EEC) of the European Water Framework Directive (2000/60/EC) calls for a discharge limit of 10 mg-N-L⁻¹ in ecologically sensitive areas [3]. Over past decades, the electrochemical oxidation of ammonia has been intensively studied for applications in fuel cells, hydrogen generation, sensors, and wastewater remediation [4,5]. Since ammonia, with low reduction potential, is

E-mail addresses: mcdyessjin@gmail.com (Y.-J. Shih), huang@udel.edu (C.P. Huang).

anodically oxidized to nitrogen gas on some noble metals, it can be integrated with a cathodic oxygen reduction to fulfill a spontaneous redox reactions and electrical energy generation [6–8]. Platinumbased materials, such as in the forms of nanoparticles, crystals with specific plane, and alloys, are normally used for ammonia electro-oxidation in alkaline media [9,10]. The primary concern of electrochemical ammonia oxidation as an environmental remediation process lies in the complicated selectivity of ammonia conversion to nitrogen gas, nitrite, and nitrate due to its multistep electron transfer and dimerization reaction.

Although the well-known biological process of Anammox[®] is effective in treating wastewaters involving the bacterial phylum *Planctomycetes*, it requires large land space and long process time compared to chemical methods [11]. In light of the technology maturity of ammonia oxidation in the energy field, intuitively, electrocatalysis may be a feasible alternative to microbial transformation such as the Anammox[®] process. At the present, there are very few investigations on the ability of electrodes made of low-cost transition metals/metal oxides for ammonia removal [12]. Indirect electrochemical ammonia oxidation has been attempted by the *in-situ* generation of active chlorine on dimensionless stable

^{*} Corresponding author.

^{**} Corresponding author.

anodes, DSA, (e.g., Ti/IrO₂, RuO₂) [13,14]. Chloramination produces several chloramines and finally gaseous nitrogen depending upon the Cl₂/NH₄-N ratio in the electrolytic cell [15,16]. However, the breakpoint chlorination potentially creates halogenated byproducts, i.e. disinfection byproducts, DBPs, which are highly toxic to humans

Ni is widely used in rechargeable alkaline batteries and supercapacitors, since the half-cell reaction of Ni(OH)2/NiOOH has a reduction potential of 0.49 V (vs. NHE) [17]. Therefore, proper control of the charging overpotential can convert the oxidized thin Ni^(II) (OH)₂ film on the metallic nickel surface to oxyhydroxide (Ni(III)OOH), which has been used to electrocatalytically oxidize some small organic compounds, such as glucose to glucolactone [18]. Voltammetry of Ni/Ni(OH)₂ in the presence of ammonia has been studied [19]. However, information on electrochemical variables that control the capability of nickel foam electrode for direct ammonia oxidation in wastewater is still limited. Several methodologies have been developed to practically treat or recover NH₄/ NH₃ dependent on ammonia concentration. For examples, at high ammonia concentration, i.e., 2000 mg/L, ammonia was recovered as struvite (MgNH₄PO₄) from wastewater by crystallization [20]. Air stripping at ammonia concentration of >500 mg/L has been attempted [21]. Anaerobic oxidation, specifically, Anammox[®], has been suggested for the treatment of ammonia containing wastewater at concentration of 200 mg/L [22]. When the concentration is > 100 mg/L, ion exchange is appropriate for the removal of ammonia from water [23]. Ammonia oxidation by chlorination has been studied at concentration <50 mg/L [16]. The total nitrogen (TN) varies over a wide range of concentration depending on the source of wastewater/water, for instance, > 1000 mg-N/L in landfill leachate [20], 300-1000 mg-N/L in pharmaceutical wastewaters [24], 250 mg-N/L from the manufacturing of semiconductor industrial wastewaters [25], and <5 mg-N/L in aquaculture effluents [26]. Our recent research has demonstrated that nickel oxide formed in-situ on Ni foam substrate during electrolysis could efficiently mediate the electron transfer of ammonia in dilute concentration (e.g., 20 mg/L) [27]. In order to demonstrate the ability of direct electro-oxidation of ammonia in aqueous solution toward nitrogen selectivity, this work aims to design a batch electrolytic cell consisting of nickel foam anode and Ti/IrO2 cathode for investigating the electrochemical oxidation of ammonia in an initial NH₃ concentration range from 50 to 450 mg-N/L. Effects of solution pH, temperature, and current density on the rate of ammonia oxidation and evolution of byproducts (nitrate, nitrite, and nitrogen gas) were evaluated based on the current efficiency, rate law, and selectivity of ammonia conversion.

2. Materials and method

2.1. Chemicals

The ammonia solution was prepared with ammonium sulfate ((NH₄)₂SO₄, J.T. Baker, USA). Sodium sulfate (Na₂SO₄, Sigma-Aldrich Co., USA) was used as supporting electrolyte. The solution pH was adjusted to a specific value with sodium hydroxide (NaOH, Merck KGaA, Germany) and sulfuric acid (H₂SO₄, 95%, Sigma-Aldrich Co., USA). Chemicals for the analysis of electrochemical intermediates included sodium nitrite (NaNO2), sodium hypochlorite (NaClO), N-(1-Naphthyl) ethylenediamine dihydrochloride (C₁₀H₇NHCH₂CH₂NH₂·2HCl), sulfanilamide (H₂NC₆H₄SO₂NH₂), and sodium phenoxide (NaOC₆H₅·3H₂O) (Sigma-Aldrich Co., USA), potassium nitrate (KNO₃) and sodium nitroprusside (Na₂ [Fe(CN)₅NO]) (Riedel-deHaën AG. Germany), ethvlenediaminetetraacetic acid disodium salt dihydrate (C₁₀H₁₄N₂Na₂O₈·2H₂O, EDTA-Na₂) (U&I Bio-Tech, Inc., USA). All reagents were of analytical grade and used without purification. The deionized water, for the preparation of all solutions, was purified with a laboratory-grade RO-ultrapure water system (resistivity > 18.18 M Ω cm).

2.2. Experimental apparatus and procedure

Electrochemical experiments were carried out with a potento-stat (CHI611C, CH Instruments, Inc., USA). A nickel foam (sheet, thickness = 2 mm, area density ~ 250 g/m², holes number = 94 ± 10 pores per linear inch (PPI), Innovation Materials Co., Ltd., Taiwan) was the working electrode. The counter electrode was an iridium oxide-coated titanium (Ti/IrO₂) and the reference electrode was Hg/HgO/1 M NaOH ($E^0 = 0.14$ V vs. NHE) (RE-61AP, ALS Co. Ltd., JAPAN). Prior to all experiments, the nickel foam was degreased with acetone (99.5%), acid-etched in 3 M H₂SO₄ for 10 min, and then rinsed with deionized water in an ultrasonic bath. Batch ammonia oxidation experiments were performed in constant current mode. Fig. 1 shows the configuration and specification of electrolytic apparatus. Two concentric nickel electrodes, with diameter of 4 and 6 cm individually and submerging in the electrolyte at a depth of

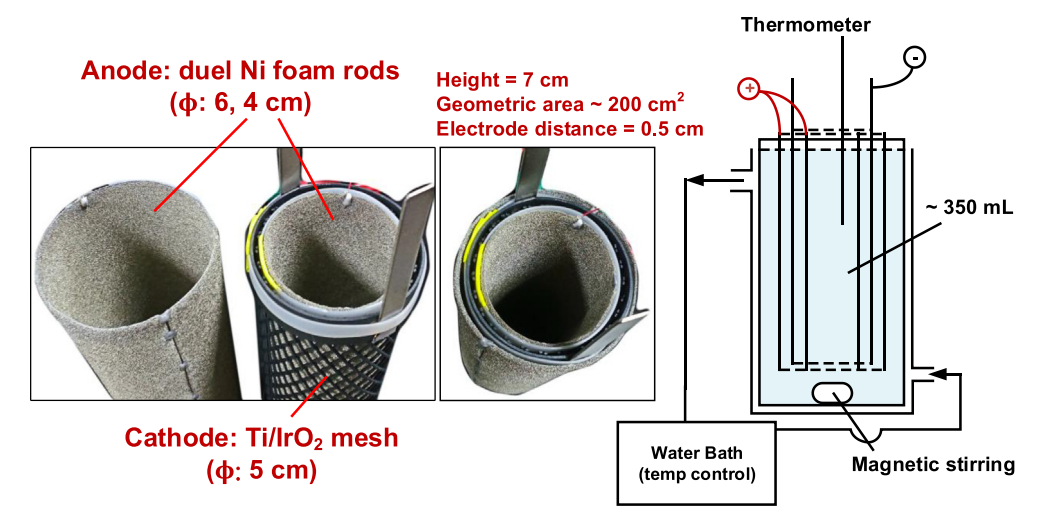


Fig. 1. Batch apparatus of electrochemical oxidation of ammonia.

7 cm, were used as the anode (total effective area ~200 cm²). A Ti/IrO₂ cylinder of 5 cm in diameter, sandwiched in between the two nickel cylinders, was the cathode. The average electrode to electrode distance was 0.5 cm. To minimize the loss of nitrogen due to the volatility of ammonia at high pH, the reactor was sealed with a Teflon cover during experiment as to minimize the exposure of the liquid surface to the air. Detailed characterization of the nickel foam electrode has been reported previously [29]. All ammonia oxidation experiments were carried out with nickel foam electrodes which were prepared in situ by electrochemical formation of NiOOH phases at anodic potential of +0.8 V vs. Hg/HgO.

2.3. Chemical analysis

A flow injection analyzer (FIA, Lachat's Quik Chem 8500 Series 2, USA) was used to analyze the concentration of aqueous nitrogen species (NH₃-N, NO₃-N, NO₂-N). Measurement of ammonia was based on the indophenol method (at 630 nm) according to the Berthelot reaction, which involved reaction among phenolate, hypochlorite, and ammonia, with nitroprusside as catalyst. The total oxidized nitrogen (NO_x) was determined by reducing nitrate to nitrite (in a copperized cadmium column) prior to diazotization of nitrite with sulfanilamide followed by coupling with N-(1-naphthyl)-ethylenediamine dihydrochloride (NED). Concentration of the pink azo dye produced was then calibrated spectrophotometrically at 540 nm [28]. Nitrate concentration was the difference between NO_x and nitrite, which was determined separately. The detection limit was 0.2 µg/L for NH₃-N, and 0.25 µg/L for both NO₂-N and NO₃-N.

The micro-morphology of the electrode surface was observed with scanning electron microscopy (SEM, JSM-6700 F, JEOL Ltd., Japan). The crystallographic structure was analyzed by X-ray diffraction (XRD, DX III, Rigaku Co., Japan) operated with Cu K α source (λ = 1.5406 Å) at a scan rate of 0.06° s⁻¹ in the incidence angle range of 20–85° (2 θ).

3. Results and discussion

3.1. Electrochemistry of nickel foam

First, the redox characteristics of metallic nickel foam in solution containing ammonia nitrogen (effective area $= 3 \, \mathrm{cm}^2$) were evaluated by voltammetry in the presence of $10 \, \mathrm{mM}$ $\mathrm{Na_2SO_4}$, as inert electrolyte (at pH 11). The *i-E* response of the nickel substrate

(Fig. 2a) had a pair of peak potentials, O_1/R_1 , at an onset potential of ca. 0.6 V, which were attributed to the formation and reduction of nickel oxyhydroxide (NiOOH), as evidenced by XPS analysis in our previous work [29]. The satellite peak following the O_1 at the positive voltage scanning direction indicated the electron transfer of Ni(II) to β - and to γ -NiOOH(s), which occurred with increase in anodic current at high overpotential, *i.e.*

$$\beta - Ni(OH)_2 + OH^- \xrightarrow{Charge} \beta - NiOOH + H_2O + e^-$$
 (1)

$$\beta - NiOOH \xrightarrow{Overcharge} \gamma - NiOOH$$
 (2)

$$\gamma - NiOOH + H_2O + e^{-\frac{Discharge}{Charge}} \alpha - Ni(OH)_2 + OH^-$$
 (3)

$$\alpha - Ni(OH)_2 \xrightarrow{Aging} \beta - Ni(OH)_2 \tag{4}$$

It must be mentioned that in reaction (2) there exists a possibility that electron is transferred to elevate the oxidation state of Ni in alpha phase to higher than (III) in gamma phase based on K-edge energy shift of BaNiO₃ [30]; whereas some recent literature has pronounced oxygen oxidation as primarily responsible for the charge storage (Ni³⁺/O*-) instead of Ni(II) to Ni(IV) (Ni⁴⁺/O²⁻) through Mossbauer and XPS analyses [31,32]. Thus the main influence of overcharging on the NiOOH is to render the oxygen framework in gamma phase more disordered than that in alpha phase. We have recently reported that although Raman spectra showed distortion of the oxygen framework in NiOOH at higher overpotential, nonetheless, results of XPS analysis did not reveal the presence of Ni valence being greater than (III) during phase transition from alpha to gamma NiOOH [27]. In the ammonia solution, the peak current of Ni(OH)₂/NiOOH was increased with increase in NH₃ concentration, implying that the faradaic electron transfers of nitrogen species were mediated by the transition of Ni(OH)2 to NiOOH. In other words, the formation of surface oxide film in-situ electrochemically and the subsequent surface modification of nickel foam at a specific potential account for the oxidation of adsorbed ammonia nitrogen. The role of Ni(OH)2/NiOOH and detailed electrocatalysis has been characterized in our recent work [29].

By subtracting the background current of nickel oxidation (namely, the pseudocapacitant current) from the total current as a function of scan rate, one obtained the net NH₃ redox current. As

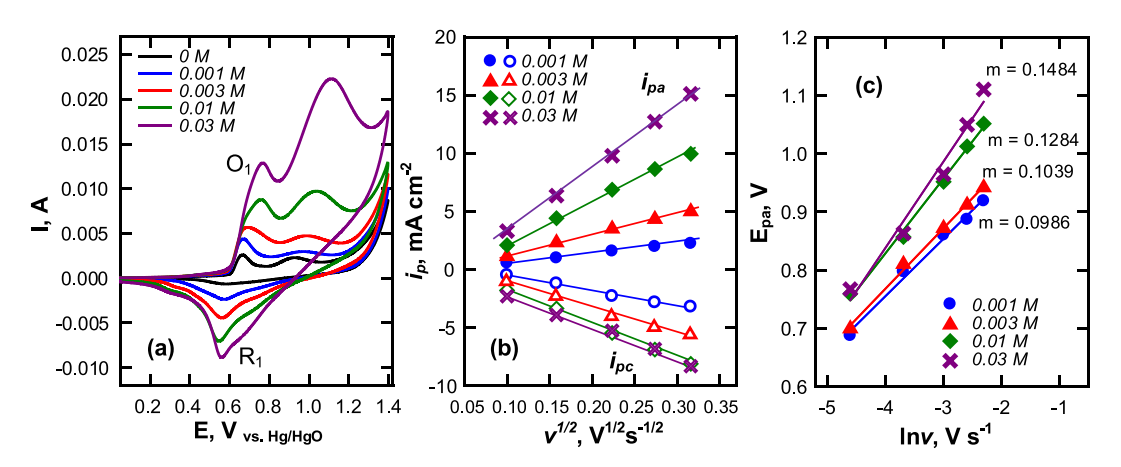


Fig. 2. (a) Analysis of cyclic voltammetry ($10 \, \text{mV} \, \text{s}^{-1}$, vs. Ag/AgCl) in the absence and presence of ammonia (pH 11, $25 \, ^{\circ}\text{C}$) using $10 \, \text{mM} \, \text{Na}_2 \text{SO}_4$ as a supporting electrolyte. (b) The corresponding net current of ammonia redox peaks as a function of $v^{1/2}$ and (c) anodic peak potential (E_{ap}) versus logarithmic scan rate ($\ln v$) in the presence of $1.0 \times 10^{-3} -3.0 \times 10^{-2} \, \text{M} \, \text{NH}_3$.

shown in Fig. 2b, both the anodic and the cathodic peak currents $(i_{pa}$ and $i_{pc})$, linearly correlated with the square root of scan rate $(\nu^{1/2})$, indicated a diffusion control reaction according to the Nicholson and Shain equation, i.e., $i_p/v^{1/2} = 2.99 \times 10^5$ n $(\alpha n_\alpha)^{1/2}D^{1/2}C$; where D is the diffusion coefficient (cm^2/sec) , C is the concentration of reactant (mol/cm^3) and αn_α is the product of transfer coefficient and the number of electron transfer involved in the rate-limiting step. Since the peak potential, E_p , is obviously dependent of the scan rate, the electron transfer process of either the oxidation of NH₃ or the reduction of intermediates (in negative voltage scan direction) appeared electrochemically irreversible. The relationship between E_p and scan rate (ν) of adsorbed species in the irreversible process can be expressed by the Laviron equation [33]:

$$E_{pa} = E^{0'} - \frac{RT}{(1-\alpha)nF} \ln \frac{RTk_s}{(1-\alpha)nF} + \frac{RT}{(1-\alpha)nF} \ln \nu$$
 (5)

Where α , n and k_s are the anodic electron transfer coefficient, the number of electrons and electron transfer rate constant, respectively. Plot of the anodic peak potential (E_{pa}) versus the logarithmic scan rate ($\ln \nu$) resulted in a straight line, which slope and intercept gave the transfer coefficient (α) and the reaction rate constant (k_s), respectively (Fig. 2c). At T = 298 K, F = 96485C/mol, and R = 8.314 J/mol-K, the term $(1-\alpha)n$ was 0.73, 0.75, 0.80, and 0.83, and k_s was 1.25, 1.29, 1.48, and 1.59 s⁻¹ for an initial NH₃ concentration of 10^{-3} , 3×10^{-3} , 10^{-2} , and 3×10^{-2} M, respectively. If the number of electron involved in the limiting step remains the same at all initial NH₃ concentrations, i.e., the mechanism of NH₃ oxidation did not change, the main effect of increasing the electrolyte concentration would be on increasing the chemical reaction rate and enhancing ammonia oxidation, when the transfer coefficient increased.

Fig. 3 shows the change in the micromorphology and X-ray diffraction pattern of the metallic Ni anodized under a constant potential of +0.8 V (vs. Hg/HgO) for 1 h, at pH 11, and in 10 mM Na₂SO₄. The blank Ni sample had an interconnected structure with

a smooth surface (Fig. 3a,b). After electro-oxidation, rougher surfaces appear on the oxidized Ni substrate (Fig. 3c), visualized as black spots, and numerous nano-whiskers of Ni(OH)2/NiOOH oxides (Fig. 3d) were created. Obviously, electrochemical oxidation increases the roughness of the nickel foam and specific surface area. which is expected to increase in ammonia oxidation. Nonetheless. according to the proposed reaction mechanism of Langmuir-Hinshelwood model (supporting data), ammonia adsorption precedes its oxidation on the electrode surface, which is the ratelimiting step. Therefore, high specific surface area facilitates ammonia adsorption but not necessarily controls its oxidation. Since the redox reactions occurring at the electrode and electrolyte interface involves a series of complex processes of activation, the formation of crystal facets or morphological features on the electrode surface can lower the energy barrier and efficiently accelerate the electron transfer process [34]. As shown in Fig. 3e, after ammonia oxidation, the oxidized Ni(OH)2 electrode exhibits diffraction planes of (001), (002) and (110) facets in lieu of the characteristic peaks of Ni(OH)₂ at 2θ of 44.8° (111), 52.2° (200), and 76.8° (220) of pure metallic Ni, which suggests full phase transformation of the anode surface layer [27].

3.2. Effect of pH

The proton concentration strongly influences the efficacy of electrochemical redox reaction when either anodic or cathodic half-cell reaction involves the transfer of hydrogen ions, H⁺. The solution pH can affect the standard reduction potential of the electrolytes and water (*i.e.* gas evolution) and the speciation of the reacting compounds in the solution and lead to different efficiency of chemical reactions of interest. Fig. 4 demonstrates the effect of pH (from 6 to 12) on concentration change of NH₃ and reaction products, i.e., NO₃, NO₂, and N₂ over the Ni foam electrode, in 10 mM Na₂SO₄ electrolyte and under constant current density of 1 mA/cm². The oxidation of ammonia proceeded rapidly at

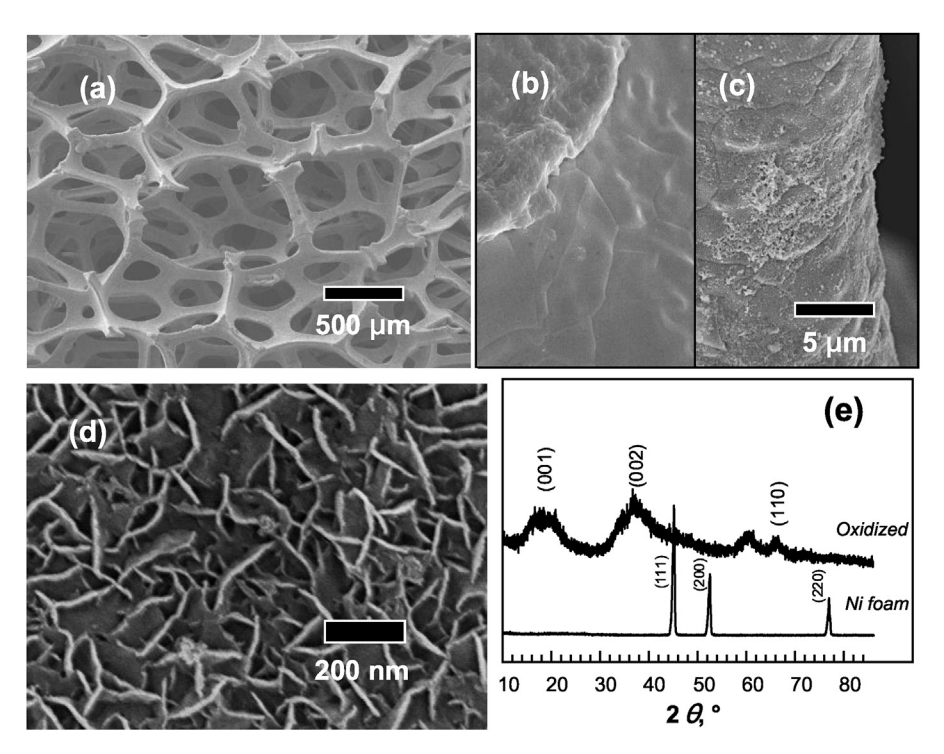


Fig. 3. SEM micromorphology of nickel foam before (a) $50 \times$, (b) $5000 \times$, and after electrochemical oxidation (c) $5000 \times$ (d) $50,000 \times$ under constant potential of +0.8 V (vs. Hg/HgO), for 1 h (pH 11, 10 mM Na₂SO₄, 10,000 \times). (e) XRD patterns of nickel foam and electrochemical oxidized sample.

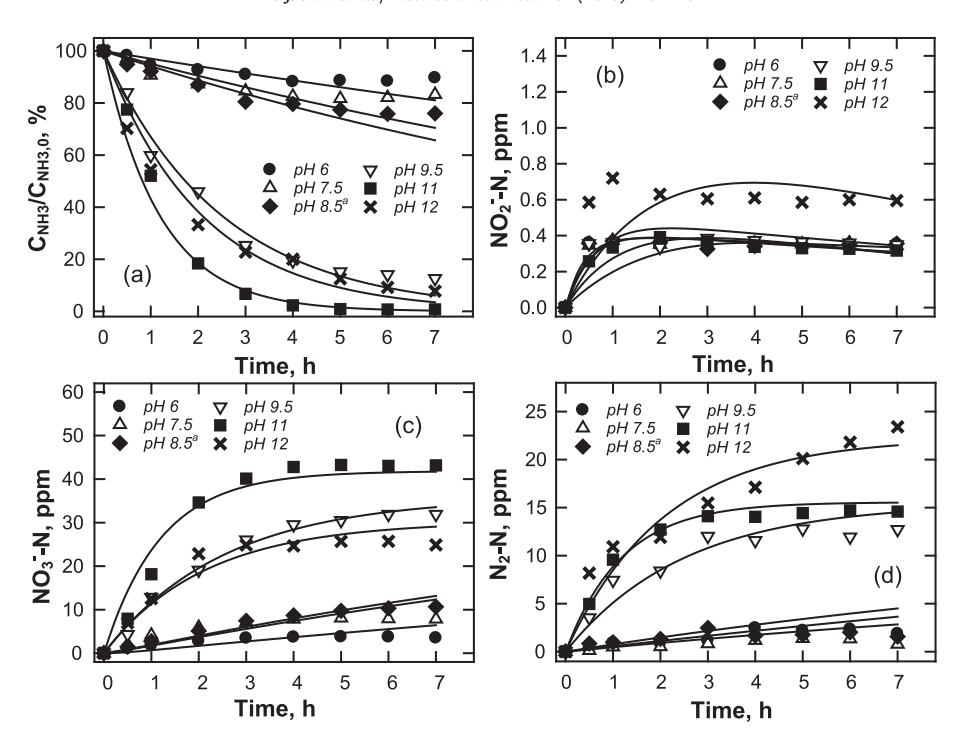


Fig. 4. Effect of pH on (a) ammonia oxidation, evolution of (b) nitrite, (c) nitrate ions and (d) nitrogen gas (electrolyte 0.01 M Na₂SO₄, NH_{3,0} = 50 ppm, current density = 1 mA/cm²) (pH 8.5 was the average value without control).

pH > 9.5, but was slow at pH < 8.5. Kapałka (2011) has reported no ammonia oxidation at neutral to acidic pH on IrO₂ electrodes [35].

Fig. 5a shows that the fraction of ammonia removal, $NH_{3,r} = (1 - [NH_{3,t}]/[NH_{3,0}]) \times 100$ (%) (red crosses), follows exactly the molar distribution fraction of NH_3 . Note that the acidity constant (pK_a) of the NH_4^+/NH_3 equilibrium is 9.25, that is, NH_3 species dominates total ammonium nitrogen (TAN) at pH > 9.25. The good fit of ammonia removal and thermodynamic distribution of NH_3 -N implies that the surface adsorbed species responsible for ammonia oxidation is primarily NH_3 not NH_4^+ as adsorption onto the anode surface is unfavorable at $pH < pK_a$ due to electrostatic repulsion. Furthermore, an increase in pH improved the selectivity of NH_3

$$(S_{Ni} = {Ni \choose NH_{3,0} - NH_{3,t}} \times 100(\%), N_i = NO_3^-, NO_2^- \text{ or } N_2) \text{ conversion}$$

toward N_2 , while inhibited NO_3^- production. Zöllig (2015) has reported that the ammonia electro-oxidation was initiated by the dehydrogenation of adsorbed ammonia and the recombination of two $NH_{x(ads)}$ to yield $N_2(g)$ [36]. Whereas, at higher oxidation potential, the formation of oxygen-containing N species dominated the selectivity of NO_x [37].

To evaluate the rate of the ammonia oxidation and production of intermediates, a steady-state approach involving adsorption/ desorption, direct electrochemical dehydrogenation, and chemical reactions among the surface species was established as shown in the Supporting Information. Briefly, the adsorbed nitrogen species, in terms surface coverage, included NH₃ (θ_{NH3}), NH₂ (θ_{NH2}), N (θ_{N}), N_2H_4 (θ_{N2H4}), N_2 (θ_{N2}), $NO_2^-(\theta_{NO2})$, and $NO_3^-(\theta_{NO3})$, which were treated as steady-state species. NH₃ and its oxidation intermediates presumably were adsorbed onto the electrode surfaces. The degree of complex formation between Ni(II) and NH3 and the accumulation of NH₃ species on the electrode surface was negligible as evident of soluble ammonia species at undetectable concentration and the weak XPS signals of N1s under working potentials of Ni oxide formation (Fig. S2). In the kinetics modeling process, there are (1) three equilibrium constants (K_1 , K_8 and K_{10}), representing the adsorption/desorption of NH₃, NO₂ and NO₃ on the electrode

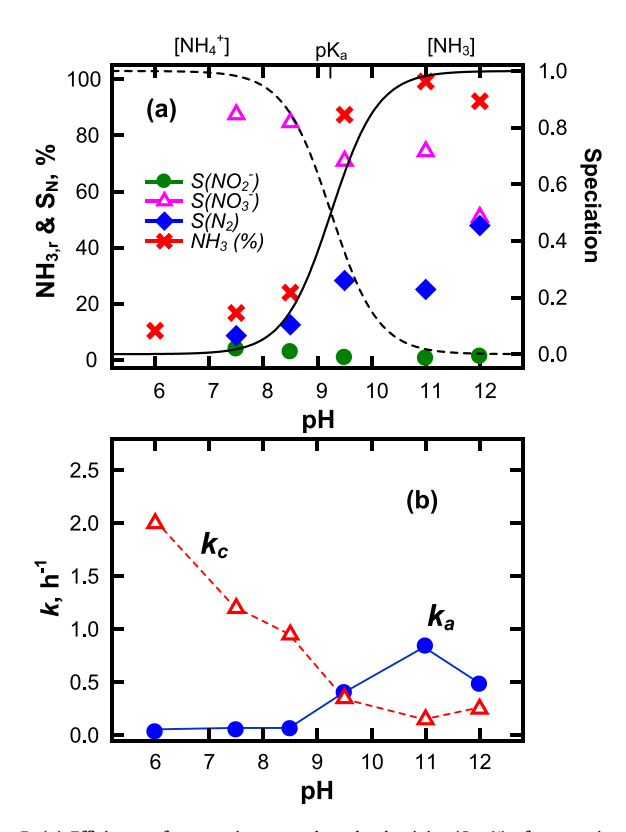


Fig. 5. (a) Efficiency of ammonia removal, and selectivity (S_N , %) of ammonia conversion to nitrite, nitrate ions and gaseous nitrogen as a function of pH over Ni foam electrode after 7 h of electrolysis; (b) rate constants k_a and k_c as a function of pH. Note that k_c and k_a are the ammonia deprotonation and nitrate production rate constants, respectively. A high k_c indicates high nitrogen selectivity.

surface, individually, (2) one equilibrium constant for NH₂ combination (K_3), and (3) five rate constants, including three for NH₃, N₂H₄ and NH₂ deprotonation (k_2 , k_4 , and k_6), respectively, and oxygenation of adsorbed N and NO $_2^-$ (k_7 and k_9), respectively, involved in the chemical reactions over surfaces of Ni foam. By considering θ_{NH2} , θ_{N} , and θ_{N2H4} as steady state species, one has the concentrations, C_{N2}, C_{NO2}, and C_{NO3} in the bulk solution.

Based on mass balance relationship, the terms, C_{NH3} , C_{N2} , C_{NO2} , and C_{NO3} were related to the initial ammonia dose, i.e., $C_{NH3,0} = C_{NH3} + C_{N2} + C_{NO2} + C_{NO3}$. The rate of ammonia depletion is equal to sum of the rate of N_2 , NO_2^- and NO_3^- generation, i.e., $-r_{NH3} = 2r_{N2} + r_{NO2} + r_{NO3}$. The following expressions were obtained (Supporting Information S3):

$$C_{NH3} = C_{NH3,0}e^{-k_a t} (6a)$$

$$C_{N2} = K_b C_{NH3,0} (1 - e^{-k_a t})$$
 (6b)

$$C_{NO2} = \frac{k_a K_d (1 - K_b)}{k_c - k_a} C_{NH3,0} \left(e^{-k_a t} - e^{-k_c t} \right)$$
 (6c)

$$\begin{split} C_{NO3} &= \frac{(1-K_b)(k_cK_d-k_aK_e+k_cK_d)}{k-k_a}C_{NH3,0}\Big(1-e^{-k_at}\Big) \\ &- \frac{k_aK_d(1-K_b)}{k_c-k_a}C_{NH3,0}(1-e^{-k_ct}\Big) \end{split} \tag{6d}$$

where the two apparent rate constants, $k_a = \frac{k_1^+ k_2 \theta \theta_{0H}}{k_1^- + k_2 \theta_{0H}}$ and $k_c =$ $\frac{k_8^-k_9\theta\theta_{OH}^0}{k_9\theta_{OH}^2+k_8^{+}}$ are related to the deprotonation of NH₃ and the production of NO_3^- , respectively, when the desorption of NH_3 and NO_2^- on surface sites is much faster than the corresponding electron transfer reactions (i.e. $k_1 \gg k_2\theta_{OH}$, $k_a = k_2K_1\theta\theta_{OH}$; $k_8^+ >> k_9\theta_{OH}^2$, $k_c = k_9 K_8 \theta \theta_{OH}^2$). the other hand, $K_b = \frac{k_3^+ k_4 \theta_{OH}^3}{k_4 k_3^+ \theta_{OH}^3 + k_3^- k_6 + k_4 k_6 \theta_{OH}^4}$, is determined by NH_x combination (*K*₃) and rate ratio of N_2 to N formation (i.e., k_4 and 4_6). The other two constants, $K_d=rac{k_8^+}{k_8\theta_{OH}^2+k_8^+}$ and $K_e=rac{k_8\theta_{OH}^2}{k_8\theta_{OH}^2+k_8^+}(K_d+K_e=1)$ are related to the desorption and oxidation of NO_2^- (i.e., k_8^+ and k_9), respectively. K_b , K_d , and K_e vary with experimental conditions (Supporting Information, S2, Table S1.) As indicated in Fig. 5b, with increasing pH, there is increase in k_a and decrease in k_c . The rate constants, k_c and k_a , are parallel to that of the NH₄/NH₃ speciation. At pH > pK_a, the selectivity of NH₃ conversion toward N₂ and NO₃ increases (Fig. 4a), which is evident of dominance by the NH₃ fraction (pH > 9.25). The degree of ammonia deprotonation determines the overall production of N₂.

3.3. Effect of temperature

The temperature of electrolytic cell was varied to assess the kinetics of the NH₃ oxidation over the Ni foam electrodes under a constant current density of 1.5 mA cm⁻² and pH 11 (initial [NH₃-N]₀ = 50 mg/L, 0.01 M Na₂SO₄ as an electrolyte). Fig. 6a shows the temperature dependence of rate constants k_a and k_c (i.e. Arrhenius plot). Over the Ni foam electrode, accordingly, the activation energy (E_a) of NH₃ oxidation was 6.4 kJ/mol with a corresponding activation energy of NO₃ production of 44 kJ/mol. In other words, the energy barrier for NH₃ deprotonation (the transfer of the first electron) was much smaller than that for oxidizing nitrogen to its highest oxidation states. Fig. 6b presents the profile of NH₃ oxidation and selectivity of conversion as a function of temperature; with increasing solution temperature from 20 to 40 °C, NH₃ oxidation

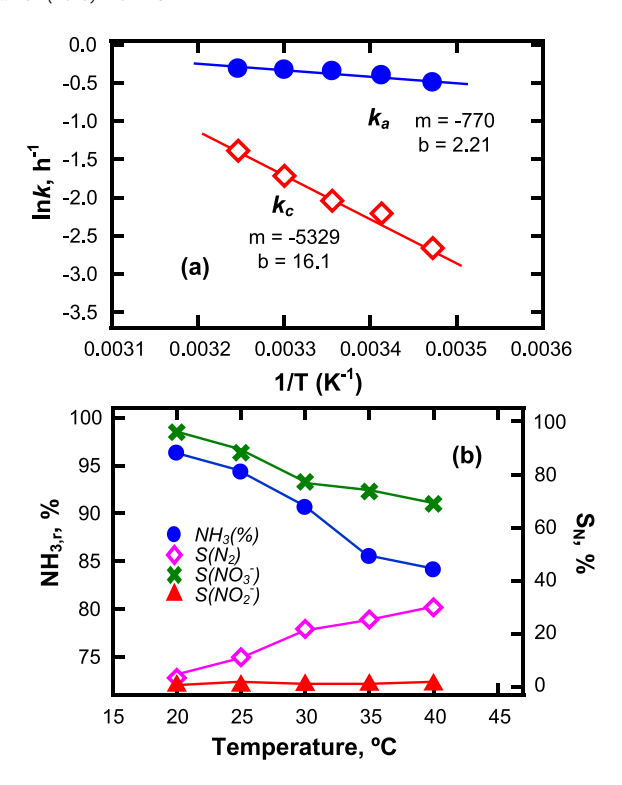


Fig. 6. (a) Arrhenius plots with rate constants of k_a and k_c ; (b) efficiency of ammonia removal (NH_{3,r}), and selectivity of ammonia conversion to nitrite, nitrate ions and gaseous nitrogen (S_N) as a function of temperature (electrolyte 0.01 M Na₂SO₄, NH_{3,0} = 50 ppm, constant current density = 1.5 mA/cm²).

and NO $_3^-$ selectivity decreased from 96 to 84% and 98 to 65%, respectively; whereas N $_2$ selectivity increased from 2 to 35%. In a typical electrolytic cell, the voltage applied, is the difference between the open circuit potential (E $_{OCP}$) and the total overpotential, η_{tot} , where η_{tot} is the overpotential sum of activation, η_{ac} , of concentration polarization, η_C , and of ohmic resistance, η_{IR} , i.e., $\eta_{tot} = \eta_{ac} + \eta_C + \eta_I$ [38]. Increasing temperature decreases the solution resistance by improving the electrolyte diffusion, reducing the term of η_{IR} and thus η_{tot} . On the other hand, E $_{OCP}$ can be modified by temperature according to the Nernst equation:

$$\Delta E_{OCP} = \Delta E^{0} - \frac{RT}{nF} \ln \left(\frac{[N_{i}]^{m} [H_{2}]^{n}}{[NH_{3}]^{x} [OH^{-}]^{y}} \right)$$
 (7)

The difference in the standard potential ($\triangle E^0$) originates from the standard Gibbs free energy of anodic ammonia oxidation and cathodic hydrogen gas evolution. Under constant current, the efficiency of NH₃ oxidation to various nitrogenous compounds is ascribed to the shift in E_{OCP}. Restated, the preference of N₂ selectivity at higher temperature was resulted from oxidizing nitrogen to a relatively lower oxidation state at lower overpotential, -III to 0, rather than further to+V.

3.4. Effect of current density

Figs. 7 and 8 show NH₃ electro-oxidation and evolution of intermediates as a function of time at different current density (CD) and initial concentration of 50 and 450 mg/L, respectively. At an initial NH₃-N concentration of 50 mg/L, NH₃ removal increased significantly with increase in CD. The concentration of NO₃ and N₂ also increased with increase in CD, except nitrite, which concentration was small and appeared to be rather unaffected by CD. NH₃ removal reached 98.5% in 7 h at CD 1.5 mA/cm². Further increase in

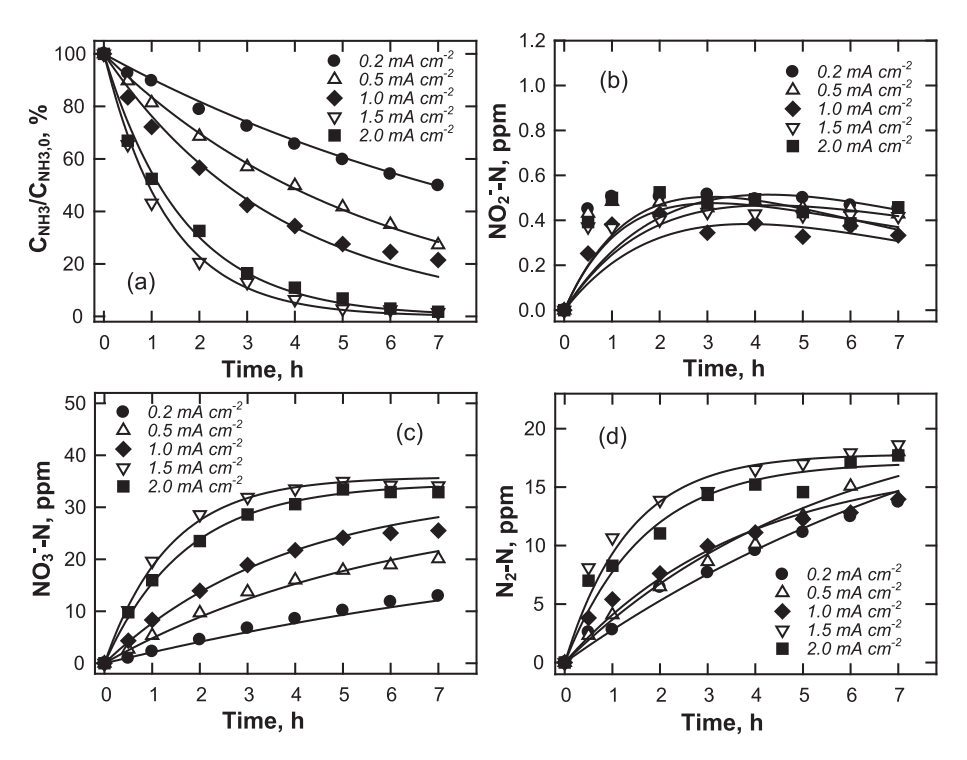
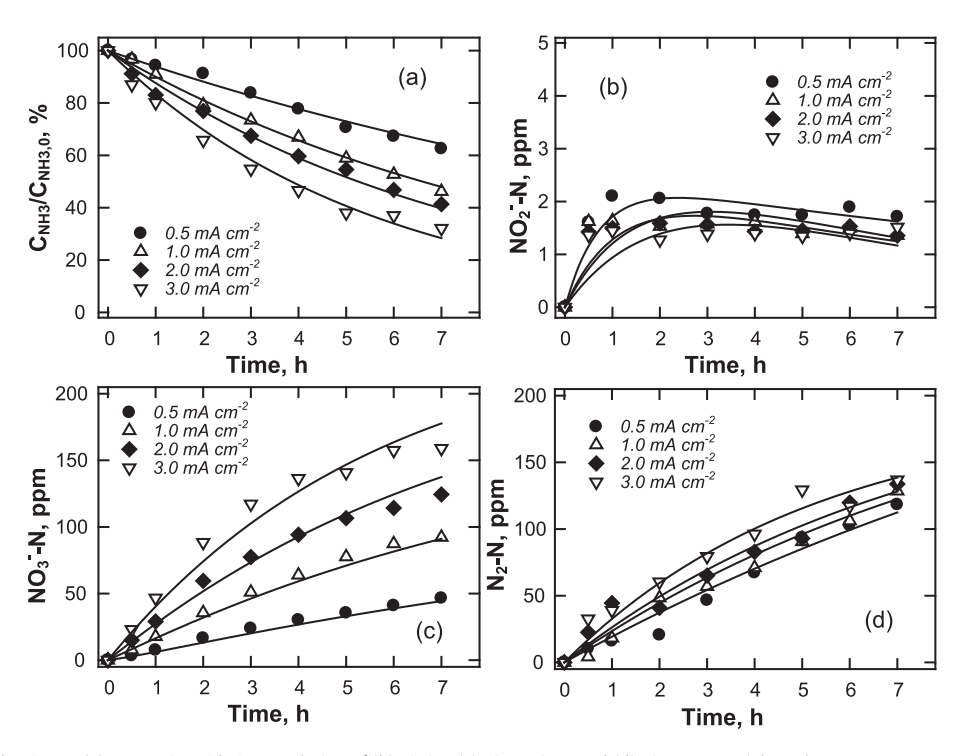


Fig. 7. Effect of current density on (a) ammonia oxidation, evolution of (b) nitrite, (c) nitrate ions and (d) nitrogen gas (electrolyte 0.01 M Na₂SO₄, NH_{3.0} = 50 ppm, pH 11).



 $\textbf{Fig. 8.} \ \ \text{Effect of current density on (a) ammonia oxidation, evolution of (b) nitrite, (c) nitrate ions and (d) nitrogen gas (electrolyte 0.01 M Na_2SO_4, NH_{3,0} = 450 \, \text{ppm, pH } 11).$

CD to >1.5 mA/cm² did not increase NH₃ oxidation significantly, nor the production of N₂ or N₂, due to occurrence of limiting current. Increasing the initial concentration of NH₃-N to 450 mg/L decreased ammonia electro-oxidation under a similar CD range of 0.5–3 mA/cm². NH₃ removal dropped to 60% in 7 h at CD 2 mA/cm². The degree of N₂ production did not increase with increase in CD significantly.

Fig. 9 summarizes the effect of CD and initial NH $_3$ concentration on NH $_3$ removal, nitrogen selectivity, and rate constants k_a and k_c (from fitting data in Fig. S1 with Eqs. (6a) and (6d)). Generally, increase in CD increased NH $_3$ removal and NO $_3$ selectivity but suppressed N $_2$ selectivity regardless of initial NH $_3$ concentration. In an electrochemical cell, the effect of CD, corresponding to a cell voltage, on the selectivity of oxidizing NH $_3$ to different

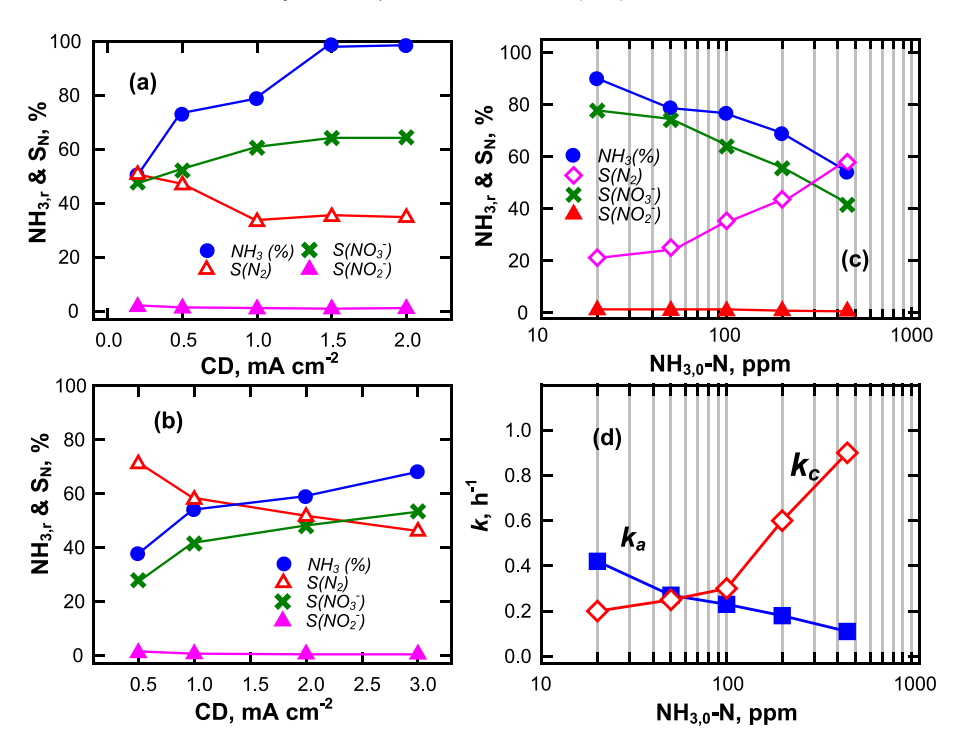


Fig. 9. Effect of current density on NH₃ removal and selectivity of NO $_2^-$, NO $_3^-$ and N₂ using initial concentrations of (a) 50 ppm and (b) 450 ppm NH₃-N (electrolyte 0.01 M Na₂SO₄, pH 11); (c) NH₃ removal, selectivity of conversion and (d) rate constants as a function of initial NH₃-N (CD = 1 mA cm⁻²).

intermediates may be attributable to the variable open circuit potentials (OCP) of corresponding chemical reactions [39]; that is,For anodic reactions:

$$N_2 + 6H_2O + 6e^- = 2NH_3 + 6OH^-$$
; $E^0 = -0.77 \text{ V (SHE)}$ (8)

$$NO_3^{-} + 6H_2O + 8e^{-} = NH_3 + 9OH^{-}; E^0 = -0.12V(SHE)$$
 (9)

and for cathodic reaction:

$$2H_2O + 2e^- = H_2 + 2OH^-; E^0 = -0.83 \text{ V (SHE)}$$
 (10)

Thus, the overall reaction for N₂ and NO₃ production could be

$$2NH_3 = N_2 + 3H_2$$
; $E_{OCP} = -0.06 \text{ V}$ (11)

$$NH_3 + 2H_2O + OH^- = NO_3^- + 4H_2$$
; $E_{OCP} = -0.71 \text{ V}$ (12)

Therefore, it is rational that at low cell voltage, corresponding to low CD, favored NH3 oxidation, with selectivity more toward N2 than NO₃, although the extent of NH₃ oxidation was not significant. Fig. 9c demonstrates the effect of initial NH_{3.0} on the electrooxidation of NH₃ and selectivity of NO₂, NO₃ and N₂ conversion under the applied constant current of 1 mA/cm². Fig. S1 shows NH₃ removal and concentration of nitrogen byproducts as a function of time. With increasing NH_{3,0} concentration, the selectivity of NO₃ significantly decreased; whereas that of N2 increased. In other words, as mentioned above, a high transfer coefficient (α) as a result of an increase in NH_{3.0} (Fig. 2c) could imply that the onset potential at ca. +0.6 V on the voltammetry was subject to the electrons involving the step of NH3 to N2 (because N2 selectivity increased with increasing NH_{3.0}). This observation also fitted the above kinetics modeling. As listed in Table S1, the equilibrium constant K_b , related to the rate ratio of N₂ to N formation over the Ni electrode, was magnified by increasing pH and initial NH₃ concentration, but was inhibited by an increase in CD. On the other hand, as predicated by effect of pH (Fig. 5b) and temperature (Fig. 6a), at low NH_{3,0}-N the selectivity of NO $_{3}^{-}$ was predominant in the oxidation of NH₃, and thus NO $_{2}^{-}$ oxidation to NO $_{3}^{-}$, at k_{c} smaller than k_{a} , was the ratelimiting step. Nevertheless, as NH_{3,0} increased, k_{c} increased and k_{a} decreased, respectively; k_{c} crossed over k_{a} at 50 mg-N/L (Fig. 9d), which implied the deprotonation of NH₃ being the rate-limiting step at higher initial ammonia concentration, NH_{3,0}-N.

Fig. 10 plots the rate constant and current efficiency against the applied current density. Here, the current efficiency, η_N , was defined as $\eta_N = nFC_NV_s/It$, where C_i is the evolving concentrations of C_{N2} , C_{NO2} , C_{NO3} in M; n is the number of transferred electrons and n, was 6, 6, and 8, for N_2 , NO_2^- , and NO_3^- , respectively; V_s is the volume of electrolyte in liter; *I* is the applied current in *A*; *t* is the reaction time in sec. The electro-oxidation constants, k_a and k_c , can obtained by fitting experimental data in Figs. 7 and 8 with Eq. (6a) - (6d). Fig. 10a shows the change of k_a and k_c as a function of CD at initial ammonia concentrations (NH_{3.0}-N) of 50 and 450 mg/L. The trend of k_a , inversely correlated to k_c in the selected range of CD, and together with results showed in Fig. 9d, clearly indicated that the rate-limiting step of NH₃ oxidation could be altered, toward N₂ or NO₃ selectivity, under a specific electrochemical condition, e.g., CD (Fig. 10a) or solution condition, specifically, initial ammonia concentration, $[NH_{3,0}]$, (Fig. 9a). In summary, a small k_0 , achieved by either increasing [NH_{3.0}] or decreasing CD, would result in a high selectivity toward N2 under which the rate of NH3 oxidation was limited by NH₃ deprotonation. The current efficiency of ammonia conversion was affected by both the applied CD and [NH_{3,0}] concentration (Fig. 10b). Considering the total charge that can be properly consumed by N_2 evolution, high η_{N2} was achieved under the condition of high [NH_{3,0}] and low CD (at the upper left corner of Fig. 10b).

The electrical energy consumption (EC, Wh/g), an evaluation of the effectiveness of electro-oxidation of ammonia over the Ni foam electrode, can be calculated by the equation: $(EC\left(\frac{Wh}{g}\right) = \frac{I \times U \times t}{\Delta[NH_3 - N]};$

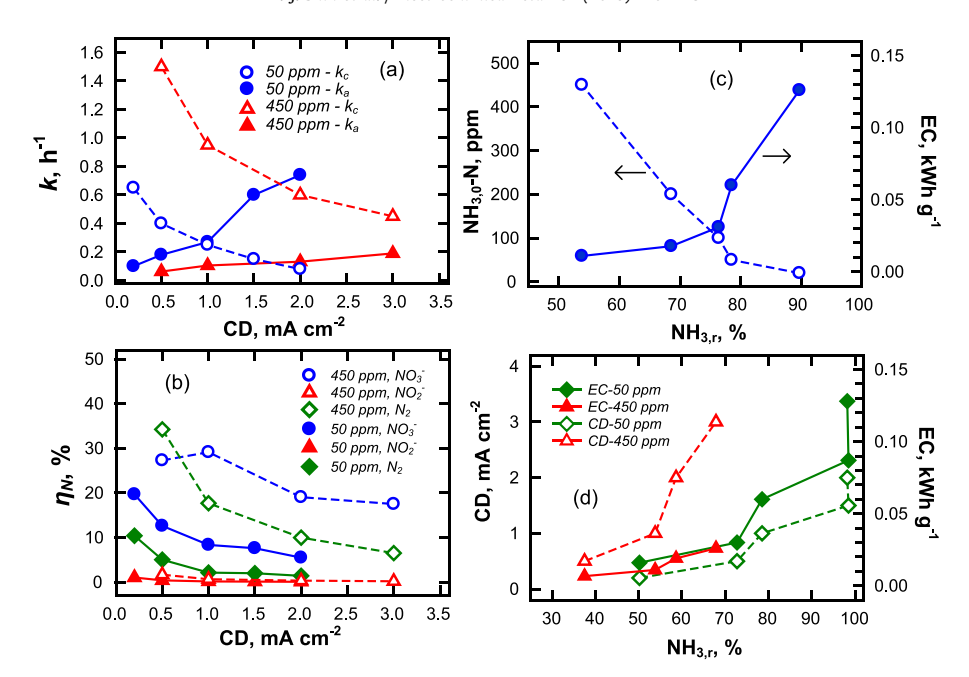


Fig. 10. (a) Rate constants k_a and k_c of ammonia conversion, and (b) current efficiencies of nitrogen intermediates evolution as a function of current density; correlations between of (c) initial concentration of NH₃ (CD = 1 mA cm⁻²) and (d) current density on the ammonia removal and energy consumption over Ni foam electrode (electrolyte 0.01 M Na₂SO₄, pH 11)

where *I* is the applied current in A, *U* is the cell voltage in volt, and $[\Delta NH_3-N]$ is the removal of ammonia nitrogen in g/L) [40]. Fig. 10c gives the plot of EC and $[NH_{3,0}]$ as a function of NH_3 removal (%). Results showed that a low $[NH_{3.0}]$ (<100 mg-N-L⁻¹) reasonably had a high ammonia removal, NH3,r, while EC significantly increased with increase in ammonia removal, NH3,r. EC increased abruptly from 30 to 130 Wh/g when NH_{3,r} was increased from 75% to 90%. As a contrast, under a fixed CD of 1 mA/cm², NH_{3,r} increased with decreasing [NH_{3.0}] almost linearly, but EC remained relatively low at ~ 20 Wh/g as $[NH_{30}] < 100 \text{ mg-N/L}$ or $NH_{3r} < 75\%$. A portion of voltage drop (IR), between the electrodes, was attributed to the conductivity of electrolyte supporting by the NH₃ concentration. Therefore, at elevated ammonia concentration, the cell voltage and EC were reduced. As shown in Fig. 10d, the effect of electrolyte conductivity on CD and EC was particularly remarkable at high $[NH_{3,0}]$ or low $NH_{3,r}$. At $NH_{3,r} < 75\%$, CD and EC remained steadily low at $[NH_{3,0}] = 450 \text{ mg-N/L}$. At $NH_{3,r} > 75\%$ EC drastically increased due to decrease in electrolyte conductivity. At NH_{3,r} >55% and $[NH_{3,0}] = 450 \text{ mg-N/L}$, CD increased exponentially with $NH_{3,r}$, due to increase in electrolyte resistance.

Contrast to the intensive interests in electrochemical hydrogen generation using high concentration of ammonia as feed solution, studies on the electrochemical treatment of ammonia contamination in aqueous solution is scarce. There are extensive interests on the development of workable anodes such as Pt/C-(SnO₂) (In₂O₃), Pt/C-(SnO₂) (Sb₂O₅), Pt/NC, Pt/Eu/C, Pt_{0.9}Ru_{0.1}/C, Ni_{1-x}Cu_xOOH for hydrogen production in ammonia solutions [9,10,41-43]. Note that the ammonia electrolyte concentration used in these galvanic cells is concentrated NH₃ (>0.5 M), which is not commonly encountered in water treatment. Indirect ammonia oxidation over boron diamond anode (BDD) in the presence of chloride salt has been attempted for the removal of total ammonia-nitrogen (TAN) from saline water [44]. The chemical oxidation demand (COD) and TAN are mineralized rather quickly, but the energy consumption is relatively high (>0.6 kWh m⁻³) due to the need of higher current density (CD > 0.3 mA cm⁻²) as to create sufficient quantity of active chlorine in lieu of simple direct ammonia oxidation. Recently we have conducted direct oxidation of ammonia over graphite-based PbO₂ electrodes, fabricated as α - and β -forms in alkaline and acidic electrolytes, respectively [45]. The selectivity of NH₃-N conversion to N₂ of the graphite-based PbO₂ electrode is relatively low compared to the nickel oxides studied in the present work.

4. Conclusions

Results clearly demonstrated the successful formation of NiOOH nano-whisker on a Ni foam substrate through a control of electrical potential. The Ni-electrode was capable of directly oxidizing NH₃ to NO₃ and N₂. The presence of NH₃ augmented the anodic current for the oxidation of metallic nickel to nickel oxyhydroxide, which suggested that the redox of Ni(II)/(III) on the surface of Ni mediated the electron transfer of ammonia nitrogen. Increasing the initial NH₃ concentration improved the transfer coefficient and favored ammonia oxidation. The surface steady-state kinetics described the pathway of NH₃ oxidation well. Under constant current mode, the selectivity of ammonia conversion was dependent on either the initial NH₃ concentration or the current density. At low current density (e.g., <1 mA cm⁻²) corresponding to a low electrode overpotential, the deprotonation of NH₃ was the rate-limiting step and the selectivity toward N₂ was favored, particularly for aqueous solution containing greater than 100 mg-N/L of initial ammonia, $[NH_{3.0}].$

Acknowledgement

The authors wish to thank The Ministry of Science and Technology (MOST) — Taiwan, for financial support of this research under Contract No. 104-2218-E-006 -020 -MY3. Addition support was provided by US NSF IOA (1632899) to CPH.

Appendix A. Supplementary data

Supplementary data related to this article can be found at https://doi.org/10.1016/j.electacta.2018.05.169.

References

- D. Kitsiou, M. Karydis, Coastal marine eutrophication assessment: a review on data analysis. Environ. Int. 37 (2011) 778–801.
- [2] G. Boczkaj, A. Fernandes, Wastewater treatment by means of advanced oxidation processes at basic pH conditions: a review, Chem. Eng. J. 320 (2017) 608–633.
- [3] M. Hauck, F.A. Maalcke-Luesken, M.S.M. Jetten, M.A.J. Huijbregts, Removing nitrogen from wastewater with side stream anammox: what are the tradeoffs between environmental impacts? Resour. Conserv. Recycl. 107 (2016) 212–219.
- [4] A.F.S. Molouk, J. Yang, T. Okanishi, H. Muroyama, T. Matsui, K. Eguchi, Comparative study on ammonia oxidation over Ni-based cermet anodes for solid oxide fuel cells, J. Power Source. 305 (2016) 72–79.
- [5] Y.U. Shin, H.Y. Yoo, S. Kim, K.M. Chung, Y.G. Park, K.H. Hwang, S.W. Hong, H. Park, K. Cho, J. Lee, Sequential combination of electro-fenton and electrochemical chlorination processes for the treatment of anaerobically-digested food wastewater, Environ. Sci. Technol. 51 (18) (2017) 10700–10710.
- [6] S. Morita, E. Kudo, R. Shirasaka, M. Yonekawa, K. Nagai, H. Ota, M.N. Gamo, H. Shiroishi, Electrochemical oxidation of ammonia by multi-wall-carbonnanotube-supported Pt shell—Ir core nanoparticles synthesized by an improved Cu short circuit deposition method, J. Electroanal. Chem. 762 (2016) 29–36.
- [7] Z.F. Li, Y. Wang, G.G. Botte, Revisiting the electrochemical oxidation of ammonia on carbon-supported metal nanoparticle catalysts, Electrochim. Acta 228 (2017) 351–360.
- [8] M. Kishimoto, N. Furukawa, T. Kume, H. Iwai, H. Yoshida, Formulation of ammonia decomposition rate in Ni-YSZ anode of solid oxide fuel cells, Intern. J. Hyd. Energ. 42 (2017) 2370–2380.
- [9] V.A. Ribeiro, I.C. de Freitas, A.O. Neto, E.V. Spinacé, J.C.M. Silva, Platinum nanoparticles supported on nitrogen-doped carbon for ammonia electrooxidation, Mater. Chem. Phys. 200 (2017) 354–360.
- [10] Y. Kang, W. Wang, J. Li, C. Hua, S. Xue, Z. Lei, High performance PtxEu alloys as effective electrocatalysts for ammonia electro-oxidation, Intern. J. Hyd. Energ. 42 (2017) 18959–18967.
- [11] K. Isaka, Y. Kimura, M. Matsuura, T. Osaka, S. Tsuneda, First full-scale nitritation-anammox plant using gel entrapment technology for ammonia plant, Biochem. Eng. J. 122 (2017) 115–122.
- [12] J. Yao, M. Zhou, D. Wen, Q. Xue, J. Wang, Electrochemical conversion of ammonia to nitrogen in non-chlorinated aqueous solution by controlling pH value, J. Electroanal. Chem. 776 (2016) 53–58.
- [13] O. Lahav, R.B. Asher, Y. Gendel, Potential applications of indirect electrochemical ammonia oxidation within the operation of freshwater and salinewater recirculating aquaculture systems, Aquacul. Eng. 65 (2015) 55–64.
- [14] H. Zöllig, C. Fritzsche, E. Morgenroth, K.M. Udert, Direct electrochemical oxidation of ammonia on graphite as a treatment option for stored sourceseparated urine, Water Res. 69 (2015) 284–294.
- [15] Y. Gendel, O. Lahav, Revealing the mechanism of indirect ammonia electrooxidation, Electrochim. Acta 63 (2012) 209–219.
- [16] X. Zhang, W. Li, E.R. Blatchley, X. Wang, P. Ren, UV/chlorine process for ammonia removal and disinfection by-product reduction: comparison with chlorination, Water Res. 68 (2015) 804–811.
- [17] L. Hu, Z. Yu, Z. Hu, Y. Song, F. Zhang, H. Zhu, S. Jiao, Facile synthesis of amorphous Ni(OH)₂ for high-performance supercapacitors via electrochemical assembly in a reverse micelle, Electrochim. Acta 174 (2015), 273-181.
- [18] H. Tian, M. Jia, M. Zhang, J. Hu, Nonenzymatic glucose sensor based on nickel ion implanted-modified indium tin oxide electrode, Electrochim. Acta 96 (2013) 285–290.
- [19] A. Kapałka, A. Cally, S. Neodo, C. Comninellis, M. Wächter, K.M. Udert, Electrochemical behavior of ammonia at Ni/Ni(OH)₂ electrode, Electrochem. Commun. 12 (2010) 18–21.
- [20] S. He, Y. Zhang, M. Yang, W. Du, H. Harada, Repeated use of MAP decomposition residues for the removal of high ammonium concentration from landfill leachate, Chemosphere 66 (2007) 2233–2238.
- [21] W. Jiao, S. Luo, Z. He, Y. Liu, Applications of high gravity technologies for wastewater treatment: a review, Chem. Eng. J. 313 (2017) 912–927.
- [22] H. Li, W. Tao, Efficient ammonia removal in recirculating vertical flow constructed wetlands: complementary roles of anammox and denitrification in simultaneous nitritation, anammox and denitrification process, Chem. Eng. J. 317 (2017) 972–979.
- [23] I. Sancho, E. Licon, C. Valderrama, N. de Arespacochaga, S. López-Palau,

- J.L. Cortina, Recovery of ammonia from domestic wastewater effluents as liquid fertilizers by integration of natural zeolites and hollow fibre membrane contactors, Sci. Total Environ. 584–585 (2017) 244–251.
- [24] X. Shi, K.Y. Leong, H.Y. Ng, Anaerobic treatment of pharmaceutical wastewater: a critical review, Bioresour. Technol. 245 (2017) 1238–1244.
- [25] S. Aoudj, A. Khelifa, N. Drouiche, Removal of fluoride, SDS, ammonia and turbidity from semiconductor wastewater by combined electrocoagulation—electroflotation, Chemosphere 180 (2017) 379—387.
- [26] F. Bernardi, I.V. Zadinelo, H.J. Alvesc, F. Meurera, L.D. dos Santos, Chitins and chitosans for the removal of total ammonia of aquaculture effluents, Aquaculture 483 (2018) 203–212.
- [27] Y.J. Shih, Y.H. Huang, C.P. Huang, Electrocatalytic ammonia oxidation over a nickel foam electrode: role of Ni(OH)₂(s)-NiOOH(s) nanocatalysts, Electrochim. Acta 263 (2018) 261–271.
- [28] B.S. Gentle, P.S. Ellis, M.R. Grace, I.D. McKelvie, Flow analysis methods for the direct ultra-violet spectrophotometric measurement of nitrate and total nitrogen in freshwaters, Anal. Chim. Acta 704 (2011) 116–122.
- [29] M. Merrill, M. Worsley, A. Wittstock, J. Biener, M. Stadermann, Determination of the "NiOOH" charge and discharge mechanisms at ideal activity, J. Electroanal. Chem. 717–718 (2014) 177–188.
- [30] N.R.S. Farley, S.J. Gurman, A.R. Hillman, Dynamic EXAFS study of discharging nickel hydroxide electrode with non-integer Ni valency, Electrochim. Acta 46 (2001) 3119–3127.
- [31] R. Gottschall, R. Scho1llhorn, M. Muhler, N. Jansen, D. Walcher, P. Gutlich, Electronic state of nickel in barium nickel oxide, BaNiO₃, Inorg. Chem. 37 (1998) 1513–1518.
- [32] M. Merrill, M. Worsley, A. Wittstock, J. Biener, M. Stadermann, Determination of the "NiOOH" charge and discharge mechanisms at ideal activity, J. Electroanal. Chem. 717–718 (2014) 177–188.
- [33] M. Arvand, M.S. Ardaki, M.A. Zanjanchi, A new sensing platform based on electrospun copper oxide/ionic liquid nanocomposite for selective determination of risperidone, RSC Adv. 5 (2015), 40578–44058.
- [34] E. Bertin, S. Garbarino, D. Guay, J. Solla-Gullón, F.J. Vidal-Iglesias, J.M. Feliu, Electrodeposited platinum thin films with preferential (100) orientation: characterization and electrocatalytic properties for ammonia and formic acid oxidation, J. Power Source. 225 (2013) 323–329.
- [35] A. Kapałka, S. Fierro, Z. Frontistis, A. Katsaounis, S. Neodoa, O. Frey, N. de Rooij, K.M. Udert, C. Comninellis, Electrochemical oxidation of ammonia (NH⁺₄/NH₃) on thermally and electrochemically prepared IrO₂ electrodes, Electrochim. Acta 56 (2011) 1361–1365.
- [36] H. Zöllig, E. Morgenroth, K.M. Udert, Inhibition of direct electrolytic ammonia oxidation due to a change in local pH, Electrochim. Acta 165 (2015) 348–355.
- [37] A. Allagui, S. Sarfraz, S. Ntais, F. Al momani, E.A. Baranova, Electrochemical behavior of ammonia on Ni₉₈Pd₂ nano-structured catalyst, Int. J. Hydrogen Energ. 39 (2014) 41–48.
- [38] C.G. Lee, Effect of temperature on the cathodic overpotential in a molten carbonate fuel cell, J. Electroanal. Chem. 701 (2013) 36–42.
- [39] L.A. Diaz, A. Valenzuela-Muniz, M. Muthuvel, G.G. Botte, Analysis of ammonia electro-oxidation kinetics using a rotating disk electrode, Electrochim. Acta 89 (2013) 413–421.
- [40] P.A. Diaw, N. Oturan, M.D.G. Seye, A. Coly, A. Tine, J.J. Aaron, M.A. Oturan, Oxidative degradation and mineralization of the phenylurea herbicide fluometuron in aqueous media by the electro-Fenton process, Sep. Purif. Technol. 186 (2017) 197–206.
- [41] J.C.M. Silva, R.M. Piasentin, E.V. Spinace, A.O. Neto, E.A. Baranova, The effect of antimony-tin and indium-tin oxide supports on the catalytic activity of Pt nanoparticles for ammonia electro-oxidation, Mater. Chem. Phys. 180 (2016) 27, 102
- [42] W. Xu, R. Lan, D. Du, J. Humphreys, M. Walker, Z. Wu, H. Wang, S. Tao, Directly growing hierarchical nickel-copper hydroxide nanowires on carbon fibre cloth for efficient electrooxidation of ammonia, Appl. Catal. B Environ. 218 (2017) 470–479.
- [43] J.C.M. Silva, S. Ntais, E. Teixeira-Neto, E.V. Spinace, X. Cui, A.O. Neto, E.A. Baranova, Evaluation of carbon supported platinumeruthenium nanoparticles for ammonia electro-oxidation: combined fuel cell and electrochemical approach, Int. J. Hyd. Energ. 42 (2017) 193–201.
- [44] V. Diaz, R. Ibanez, P. Gomez, A.M. Urtiaga, I. Ortiz, Kinetics of electro-oxidation of ammonia-N, nitrites and COD from a recirculating aquaculture saline water system using BDD anodes, Water Res. 45 (2011) 125–134.
- [45] Y.J. Shih, Y.H. Huang, C.P. Huang, Oxidation of ammonia in dilute aqueous solutions over graphite-supported a- and b-lead dioxide electrodes (PbO₂@G), Electrochim. Acta 257 (2017) 444–454.